Electron transfer proteins in gut bacteria yield metabolites that circulate in the host

Yuanyuan Liu[1,2], Haoqing Chen[1,2], William Van Treuren[2], Bi-Huei Hou[1,2], Steven K. Higginbottom[2], Justin L. Sonnenburg[2,3], and Dylan Dodd[1,2†]

[1]Department of Pathology Stanford University School of Medicine, Stanford, CA, USA; [2]Department of Microbiology and Immunology, Stanford University School of Medicine, Stanford, CA, USA; [3]Center for Human Microbiome Studies, Stanford, CA, USA.

[†] Correspondence: ddodd2@stanford.edu

It has long been known that proteolytic Clostridia obtain their energy by coupling oxidative and reductive pathways for amino acid metabolism – the Stickland reaction[1]. The oxidation of one amino acid is coupled with reduction of another, yielding energy in the former step and re-achieving redox balance with the latter. Here, we find that the gut bacterium, *Clostridium sporogenes* metabolizes amino acids through reductive pathways to produce metabolites that circulate within the host. Measurements *in vitro* indicate that reductive Stickland pathways are coupled to ATP formation, revealing their role in energy capture by gut bacteria. By probing the genetics of *C. sporogenes*, we find that the Rnf complex is involved in reductive amino acid metabolism. Rnf complex mutants are attenuated for growth in the mouse gut, demonstrating the importance of energy capture during reductive metabolism for gut colonization. Our findings reveal that the production of high-abundance molecules by a commensal bacterium within the host gut is linked to an energy yielding redox process.

26 Proteolytic Clostridia are a group of anaerobic bacteria that have the unique ability to
27 grow with amino acids and peptides as their sole energy source. These microbes
28 colonize the gastrointestinal tract of mammals where their metabolic end products
29 accumulate within the gut[2-4] and are absorbed into circulation mediating important
30 effects on host health[5]. Amino acid metabolites like indolepropionate, 3-(4-
31 hydroxyphenyl)propionate, and indoleacetate are drug-like small molecules that bind
32 host receptors and modulate physiology including intestinal permeability[6,7] and immune
33 homeostasis[8,9]. Amino acid metabolites also mediate syntrophic metabolic interactions
34 among microbes within the gut, with aryl and branched chain fatty acids being required
35 growth factors for several groups of anaerobic gut bacteria[10-12]. Despite their importance
36 to human health and disease, we know very little about the metabolic processes gut
37 bacteria employ to produce such molecules.

38

39 ***Amino acid metabolism by Clostridium sporogenes***

40 Here we used the gut bacterium, *Clostridium sporogenes* as a model to probe the
41 origin of amino acid metabolites produced within the gut and that circulate in the host.
42 *C. sporogenes* grows rapidly under anaerobic conditions in a defined medium
43 containing a mixture of free amino acids and glucose, achieving a doubling time of ~37
44 minutes (**Extended data Fig. 1a**). After 24 h of growth, most amino acids were depleted
45 from the medium (**Extended data Fig. 1b**) and a total of fifteen different metabolites
46 accumulated in culture supernatants (**Extended data Fig. 1c**). Early studies with *C.*
47 *sporogenes* revealed that it metabolizes amino acids in pairs, coupling the oxidation of
48 one with the reduction of another (the Stickland Reaction)[13]. To assess the degree to

49 which *C. sporogenes* utilizes amino acids as Stickland pairs, we performed a high
50 throughput growth-based assay. Cells were grown in a basal medium containing ten
51 essential amino acids (1 mM each) with higher concentrations (25 mM each) of amino
52 acids or glucose individually or in pairs and growth was monitored
53 spectrophotometrically. The results from these experiments are presented in **Extended**
54 **data Fig. 2** and summarized in the **Supplementary Text**. Results from these growth-
55 based assays support the following conclusions: 1) Specific pairs of amino acids
56 function synergistically to promote the growth of *C. sporogenes* (Stickland metabolism).
57 2) Reductive pathway substrates including proline and amino acids that converge on
58 proline (e.g., *trans*-4-hydroxyproline, arginine, citrulline, and ornithine) stimulate growth
59 yields from glucose. 3) *C. sporogenes* utilizes serine in a manner similar to glucose,
60 coupling it to reductive pathway substrates to achieve high growth yields. 4) Proline and
61 *trans*-4-hydroxyproline both stimulated growth yield with branched chain amino acids
62 (valine, isoleucine, and leucine), but this required supplemental acetate presumably for
63 anabolic purposes.

64

65 ***C. sporogenes produces amino acid metabolites that circulate in the host***

66 To evaluate how *C. sporogenes* influences metabolites that circulate within the host,
67 we colonized germ-free mice with *C. sporogenes* and quantified metabolites in feces,
68 cecal contents, plasma, and urine using stable isotope dilution liquid chromatography –
69 mass spectrometry (LC-MS) (**Supplementary Tables 1-4**). Of the 15 metabolites
70 detected in cultures of *C. sporogenes* (**Extended data Fig. 1c**), 13 were present in the
71 feces of *C. sporogenes* colonized mice one week after colonization (**Fig. 1a**)

72 demonstrating that *C. sporogenes* produces these metabolites *in vivo*. In plasma, we
73 found four metabolites that were elevated in colonized vs. germ-free mice, which
74 included 5-aminovalerate, phenylpropionate, 3-(4-hydroxyphenyl)propionate, and
75 indolepropionate (**Fig. 1a**). The remaining nine compounds present in feces, but absent
76 in plasma are likely either excreted in feces or absorbed and metabolized by the host.
77 To confirm that these circulating metabolites arise from bacterial metabolism in the gut,
78 we colonized germ-free mice with *C. sporogenes* and treated separate groups with or
79 without oral antibiotics (**Fig. 1b**). Following colonization, the four circulating metabolites
80 achieved mean plasma concentrations ranging from ~3 μM for phenylpropionate to
81 ~100 μM for indolepropionate (**Fig. 1c**). After antibiotic treatment, the plasma levels of
82 all four metabolites were reduced to undetectable levels (**Fig. 1c**), demonstrating their
83 dependence on bacterial metabolism in the gut. In urine, we observed similar trends for
84 5-aminovalerate, phenylpropionate, and 3-(4-hydroxyphenyl)propionate, with their levels
85 rising after colonization and falling after antibiotic treatment; however, indolepropionate
86 was undetectable in all urine samples (**Supplementary Table 3**). Using a combination
87 of untargeted metabolomics, tandem mass spectrometry (MS/MS), and comparison with
88 authentic standards, we identified high levels of indolepropionylglycine (IPGly) in the
89 urine of *C. sporogenes* colonized mice (**Extended data Fig. 3**) that tracked with plasma
90 levels of indolepropionate (**Fig. 1c**), suggesting that IPGly is the excreted form of
91 indolepropionate.

92 Having identified four *C. sporogenes* dependent circulating metabolites in
93 gnotobiotic mice, we next asked whether these compounds are present in human blood.
94 To test this, we obtained 99 plasma samples from healthy human blood donors and

95 quantified metabolites using LC-MS (**Supplementary Table 5**). Of the four metabolites,
96 indolepropionate was the most prevalent, being detected in the blood of 99% of
97 individuals (**Fig. 1d**). Consistent with our analysis of gnotobiotic mice (**Fig. 1c**),
98 indolepropionate concentrations were also the highest, ranging in human plasma from
99 230 nM to 9.3 μM (**Fig. 1d**). After repeated analyses, one individual was confirmed to
100 have high plasma indolepropionate levels of 110 μM. Phenylpropionate and 5-
101 aminovalerate were also detected in the majority of healthy blood donors, whereas 3-(4-
102 hydroxyphenyl)propionate levels were lower and present in less than half of individuals
103 (**Fig. 1d**). Collectively, these findings demonstrate that amino acid metabolism within
104 the gut yields metabolites that circulate within the host. Of these metabolites,
105 indolepropionate is the most concentrated in both gnotobiotic mice and in humans, with
106 rare individuals having high concentrations of circulating indolepropionate.

107

108 ***Circulating metabolites are products of reductive Stickland metabolism***

109 We next sought to understand the metabolic processes that underlie production of
110 these four circulating metabolites. *C. sporogenes* metabolizes amino acids in pairs,
111 coupling the oxidation of one with the reduction of another via the Stickland Reaction.
112 Oxidative pathways are thought to yield ATP via substrate level phosphorylation, and
113 reductive pathways provide redox balance within the cell (**Fig. 2a**)[1,14]. In this context,
114 previous studies have indicated that 5-aminovalerate, phenylpropionate, 3-(4-
115 hydroxyphenyl)propionate, and indolepropionate are end products of reductive Stickland
116 metabolism of Pro, Phe, Tyr, and Trp, respectively[6,15].

117 To test whether these four circulating metabolites arise from metabolism of their
118 cognate amino acids, we performed stable isotope tracing experiments. *C. sporogenes*
119 was cultured in a defined medium containing all 20 proteinogenic amino acids (1 mM
120 each) and glucose (10 mM) where Pro, Phe, Tyr, or Trp were individually substituted by
121 their deuterium isotopologues (Pro-d7, Phe-d8, Tyr-d4, or Trp-d5) and metabolites were
122 measured by LC-MS during growth. Under these conditions, cells reached maximal
123 optical densities of ~0.5 by 16 h. Labeled Pro, Phe, and Tyr were completely consumed
124 by 24 h, being converted to labeled derivatives (5-aminovalerate-d6,d5;
125 phenylpropionate-d7,d6,d5; and 3-(4-hydroxyphenyl)propionate-d4) with yields ranging
126 from 65%-109% (**Fig. 2b**). Trp metabolism was comparably slower, but ~93% of Trp
127 was consumed by 24 h, being converted to indolepropionate-d5 with a yield of 60%
128 (**Fig. 2b**). Despite pathways existing in *C. sporogenes* for the oxidative metabolism of
129 Phe, Tyr, and Trp[6,16], under these experimental conditions only reductive products of
130 these amino acids were detected (**Fig. 2c**). These findings indicate that *C. sporogenes*
131 cells convert the majority of these amino acids to reduced products, rather than using
132 them for biosynthetic purposes such as protein synthesis. In cultures where labeled
133 Phe, Tyr, and Trp were provided, no unlabeled phenylpropionate, 3-(4-
134 hydroxyphenyl)propionate, or indolepropionate was detected (**Extended data Fig. 4a-c**)
135 suggesting that these metabolites arise from catabolism of their cognate amino acids,
136 not through *de novo* biosynthetic pathways from other precursors. 5-aminovalerate was
137 an exception, however, with its unlabeled product accumulating in cultures where
138 labeled Pro was added (**Extended data Fig. 4d**), which we found reflected the capacity

139 of cells to convert Arg in the medium to proline and 5-aminovalerate (**Extended data**
140 **Fig. 4e**)[17].

141 During Stickland metabolism, the oxidation of one amino acid is coupled to the
142 reduction of another, resulting in stimulatory effects of amino acid pairs[1]. Next, we
143 sought to test whether production of the reductive metabolites, 5-aminovalerate,
144 phenylpropionate, and indolepropionate is stimulated by provision of an oxidative amino
145 acid partner. Cell suspensions of *C. sporogenes* were incubated with isotopically
146 labeled amino acids (Pro, Phe, Trp) in the presence or absence of an oxidative
147 Stickland amino acid (Val) and metabolism was monitored by LC-MS. Whereas cells
148 incubated with Pro or Val alone showed limited substrate consumption and product
149 accumulation (**Fig. 2d**), cells incubated with both Pro and Val consumed most of the Pro
150 and all the Val by 3h, converting Pro to 5-aminovalerate and Val to isobutyrate (**Fig.**
151 **2d**). Similar results were seen with the Phe/Val combination (**Fig. 2d**), however the
152 Trp/Val combination yielded a more subtle pattern, where indolepropionate production
153 was low (**Fig. 2d**), but significantly higher when Val was added (**Extended data Fig. 5**).
154 Collectively, these findings demonstrate that 5-aminovalerate, phenylpropionate, 3-(4-
155 hydroxyphenyl)propionate, and indolepropionate are reductive pathway products of
156 coupled Stickland reactions by gut bacteria.

157

158 ***Reductive Stickland metabolism is coupled to ATP formation***

159 During Stickland metabolism of amino acids, oxidative pathways are thought to yield
160 ATP via substrate level phosphorylation, and reductive pathways provide redox balance

161 within the cell[1,14]. However, anaerobic bacteria can also use reductive metabolism to
162 fuel anaerobic respiration, providing an additional mechanism to obtain energy.
163 Examples include fumarate reduction by *Bacteroides fragilis* (involved in carbohydrate
164 metabolism)[18], caffeate respiration by *Acetobacterium woodii*[19] and cinnamate reduction
165 by *C. sporogenes*[20] (involved in metabolism of plant secondary metabolites), and
166 reductive acetogenesis by *C. ljungahlii*[21]. We reasoned that reductive pathways for
167 amino acid metabolism via the Stickland reaction might also serve a role in energy
168 capture for bacteria within the gut. A previous study demonstrated that Pro reduction in
169 *C. sporogenes* is linked to vectorial transmembrane proton translocation[22], however
170 whether this proton gradient is coupled to ATP synthesis is unknown. Furthermore, it is
171 not known whether additional pathways for reductive amino acid metabolism are
172 involved in energy capture. Therefore, we analyzed the metabolic gene clusters
173 encoding reductive amino acid pathways with an eye towards identifying potential
174 mechanisms for energy capture.

175 Inspection of the gene clusters encoding reductive amino acid pathways revealed
176 that each pathway converges on a step involving a multi-subunit electron transfer
177 protein (**Fig. 3a**). The aryl amino acid reductive gene cluster encodes an acyl-CoA
178 dehydrogenase with two electron transfer factors (EtfAB) sharing 40-60% amino acid
179 identity with the butyryl-CoA dehydrogenase-EtfAB (Bcd) complex from *Clostridium*
180 *kluyverii* involved in ethanol fermentation[23] (**Fig. 3b**). Bcd catalyzes flavin based
181 electron bifurcation where the energetically downhill reduction of crotonyl-CoA by NADH
182 drives the energetically uphill reduction of ferredoxin by NADH[24,25]. In so doing, the cell
183 has low-potential reduced ferredoxin at its disposal to drive ion translocation through the

184 Rnf complex with NAD^+ as an electron acceptor[26]. The gene cluster for reductive
185 leucine metabolism, present in *C. sporogenes*[27], also encodes a homolog of the Bcd
186 complex (**Fig. 3b**). The proline reductive gene cluster encodes a different electron
187 transfer protein involving the enzyme proline reductase (**Fig. 3c**). However, a link to
188 energy conservation for proline reductase has not been established. Thus, these
189 metabolic gene clusters suggest that reductive Stickland pathways may be linked to
190 ATP synthesis in the cell.

191 To test this experimentally, we established a whole cell-based ATP assay using
192 resting late log-phase cell cultures of *C. sporogenes*. Following incubation with
193 substrate, cells were quenched and permeabilized with DMSO, then ATP levels were
194 detected by luminescence and normalized to total cellular protein levels. We validated
195 our assay by analyzing ATP formation from *trans*-cinnamate, a plant derived substrate
196 previously thought to be involved in reductive phenylalanine metabolism (**Extended**
197 **data Fig. 6, Supplementary Text**). Because Phe, Tyr, Trp, and Leu may also be
198 metabolized down oxidative pathways, we supplied cells with pathway intermediates
199 (e.g., phenyllactate, 3-(4-hydroxyphenyl)lactate, indolelactate, 2-hydroxyisocaproate)
200 specific to reductive pathways. When Pro or reductive pathway intermediates for Phe,
201 Tyr, Trp, or Leu were added to cells, ATP levels rose rapidly, plateaued, and then
202 returned to resting levels (**Fig. 3e**). Because reductive arylamino acid metabolism (Phe,
203 Tyr, Trp) operates through a shared pathway, we chose to further explore ATP
204 formation using Phe metabolism as a representative for this pathway. These analyses
205 revealed that D-phenyllactate (and not its L-stereoisomer) supported ATP formation
206 (**Extended data Fig. 7a**), being converted almost quantitatively to the reductive

207 pathway product, phenylpropionate (**Extended data Fig. 7b**). Metabolic products
208 (**Extended data Fig. 7c**) of reductive or oxidative pathways failed to elicit ATP
209 formation (**Extended data Fig. 7d-e**). Genetic disruption of acyl-CoA dehydrogenase
210 (AcdA) abolished ATP formation from DL-phenyllactate, indicating that this enzyme is
211 critical for ATP formation during reductive Phe metabolism (**Extended data Fig. 7f**).
212 Similar results were seen for metabolism of the Tyr and Trp metabolic intermediates
213 (DL-4-hydroxyphenyllactate and DL-indolelactate), with the *acdA* mutant being deficient
214 in ATP formation from these substrates (**Extended data Fig. 7g-h**). Pre-treatment of
215 cells with the protonophore, 3,3′,4′,5-tetrachlorosalicylanilide (TCS) uncoupled DL-
216 phenyllactate and proline metabolism from ATP formation (**Extended data Fig. 8**),
217 indicating that a proton gradient is involved in ATP formation. Taken together, these
218 experiments reveal that pathways for reductive Stickland metabolism are linked to ATP
219 formation and involve the generation of a proton motive force.

220

221 ***The Rnf complex is important for reductive metabolism and competition within***
222 ***the gut***

223 Having demonstrated that reductive metabolism is coupled to ATP formation, we
224 next asked whether the Rnf complex might be an important coupling site. We identified
225 a gene cluster which encodes the Rnf complex in *C. sporogenes* (**Fig. 4a**) and targeted
226 genes encoding two separate subunits (*rnfB* and *rnfE*) for disruption (**Fig. 4b**). These
227 mutants suffered a growth defect when grown in minimal medium containing 10 amino
228 acids (**Fig. 4c**), yet this phenotype could be suppressed by the addition of glucose to
229 the culture medium (**Fig. 4c**). These data suggest that the growth phenotype in *rnfB* and

230 *rnfE* mutants is characterized by defective amino acid metabolism. Metabolic profiling of
231 culture supernatants revealed that the *rnfB* mutant was defective in production of the
232 reductive pathway metabolites 5-aminovalerate, phenylpropionate, 3-(4-
233 hydroxyphenyl)propionate, and indolepropionate, suggesting an impairment in reductive
234 Stickland metabolism (**Fig. 4d, Extended data Fig. 9**). Thus while the Rnf complex
235 clearly plays a role in amino acid metabolism, it is unclear whether the mutant
236 phenotype is due solely to diminished ATP formation during reductive metabolism, or a
237 combined loss of regenerative functions that drive forward oxidative pathways.

238 Our findings suggest that disruption of the Rnf complex leads to altered amino acid
239 metabolism *in vitro*. Next, we asked whether energy capture through the Rnf complex is
240 important for production of reduced metabolites that circulate within the host. To test
241 this, we colonized gnotobiotic mice with either WT *C. sporogenes* or its *rnfB* mutant and
242 detected metabolites in cecal contents and plasma by LC-MS. By comparison to WT-
243 colonized mice, *rnfB*-colonized mice had significantly lower levels of indolepropionate
244 both in the cecal contents and the plasma (**Fig. 4e**), demonstrating a role for the Rnf
245 complex in production of microbiota-derived metabolites that circulate within the host.
246 To test whether energy capture involving the Rnf complex is important for competition
247 within the mammalian gut, germ-free mice were colonized with a 1:1 mixture of WT and
248 *rnfB* mutant cells and the relative proportions of the two strains in feces were
249 determined by Q-PCR over time. The *rnfB* mutant was rapidly outcompeted by the WT
250 strain, becoming nearly undetectable in feces by 7 days post colonization (**Fig. 4f**). This
251 finding was recapitulated in the presence of a more complex stably colonized microbial
252 community revealing the Rnf complex as a key fitness determinant for *C. sporogenes*

253 during colonization and persistence in the gastrointestinal tract (**Fig. 4g, Extended data**
254 **Fig. 10**). While our results suggest the Rnf complex is important for ATP formation, the
255 loss of a proton gradient that Rnf presumably creates, could influence additional
256 physiologic processes such as membrane transport and chemotaxis.

257 Intriguingly, the Rnf genes were previously identified as *in vivo* fitness determinants
258 for *Bacteroides* colonization in the mouse gut[28,29] yet were dispensable for growth in
259 defined medium[28]. This suggests that the Rnf complex, which is encoded by
260 phylogenetically diverse human gut bacteria (**Extended data Fig. 11**), may serve
261 distinct physiological roles across taxa.

262 **Conclusion**

263 Our results show that *C. sporogenes* ferments amino acids through coupled
264 oxidative and reductive pathways (the Stickland reaction), to produce metabolites that
265 accumulate in the intestinal lumen and that circulate within the host (**Fig. 4h**). In addition
266 to producing ATP via substrate level phosphorylation, reductive Stickland pathways
267 provide additional energy likely via electron transport phosphorylation. Acyl-CoA
268 dehydrogenases (Bcd/AcdA/AcdB) capture this energy via flavin-based electron
269 bifurcation, where potential energy is carried by reduced ferredoxin which then drives
270 extracellular proton (or sodium ion) transport via the Rnf complex. Homologs of the
271 electron transfer proteins described in this study are present in bacteria from 7 unique
272 Phyla and 38 different families (**Supplementary Table 6**). They are also prevalent
273 within human fecal metagenomic datasets (**Extended data Fig. 12**), suggesting these
274 mechanisms for energy capture are widespread within the gut. By reevaluating ATP
275 economy in the cell (considerations in **Supplementary Table 7**), reductive pathways

276 can account for ~40% of ATP from Stickland metabolism. This revises our
277 understanding of how amino acid degrading bacteria capture their energy and provides
278 fundamental insights into the origin of metabolites that circulate within the human body.
279

280 **Methods**

281 ***Bacterial strains and culture conditions.*** *Clostridium sporogenes* ATCC 15579
282 was obtained from the American Type Culture Collection (ATCC). It was routinely
283 cultured in reinforced clostridial medium (RCM) at 37 °C in a Coy type B anaerobic
284 chamber under an atmosphere of 5% hydrogen, 10% carbon dioxide, and 85% nitrogen.
285 All media and plasticware were pre-reduced in the anaerobic chamber for at least 24
286 hours before use. For growth measurements in defined medium, we used a previously
287 described defined minimal medium referred to as standard amino acid complete
288 medium (SACC)[15]. The *Escherichia coli* CA434 (HB101/pRK24) conjugation host was
289 routinely cultured at 30 °C in LB broth supplemented with tetracycline (12 μg mL^{-1}) to
290 ensure maintenance of the pRK24 plasmid. *E. coli* TG1 was used for routine cloning.
291 Chloramphenicol (25 μg mL^{-1}) was used for selection of pMTL007C-E2 plasmids in *E.*
292 *coli*. Organisms used in the defined community colonization included: *Clostridium*
293 *sporogenes* ATCC 15579, *Clostridium scindens* ATCC 35704, *Eubacterium rectale*
294 ATCC 33656, *Bifidobacterium breve* UCC2003, *Edwardsiella tarda* ATCC 23685,
295 *Bacteroides thetaiotaomicron* VPI-5482, and *Bacteroides vulgatus* ATCC 8482.

296 ***Plasmid construction and cloning.*** For specific gene disruptions, we used the
297 Intron targeting and design tool on the ClosTron website
298 (http://www.clostron.com/clostron2.php) using the Perutka algorithm. The intron
299 contained within the pMTL007C-E2 plasmid was retargeted to the specific sites listed in
300 **Supplementary Table 8** and were synthesized by DNA 2.0 (Menlo Park, CA).
301 Sequencing primers were synthesized by IDT DNA Technologies and are listed in
302 **Supplementary Table 8**.

303 ***Mutant generation using ClosTron.*** Intron-retargeted ClosTron plasmid DNA
304 was introduced into *C. sporogenes* by conjugation as described previously[6].
305 Transconjugants were selected on RCM agar supplemented with D-cycloserine (250 μg
306 mL^{-1}) and thiamphenicol (15 μg mL^{-1}), re-streaked for purity, and individual well-
307 isolated colonies were inoculated into RCM broth (without agar) containing the same
308 antibiotics. After overnight culture, the cells were diluted 10-fold, then 100 μL was
309 spread on an RCM agar plate containing erythromycin (5 μg mL^{-1}). These colonies
310 were picked, re-streaked onto TYG agar plates supplemented with erythromycin and
311 well-isolated colonies were inoculated into TYG broth supplemented with erythromycin.
312 Genomic DNA was isolated from candidate clones using the DNeasy Blood and Tissue
313 Kit from Qiagen with a lysozyme pre-treatment step, and this DNA was used as a
314 template for PCR using gene-specific primers. Primer sets were designed to produce a
315 ~600-bp product for the wild-type and ~2,800-bp product for the mutant containing the
316 intron. When verified mutants were streaked onto TYG plates containing thiamphenicol,
317 no growth was observed, indicating that the pMTL007C-E2 plasmid had been lost.

318 ***Monitoring bacteria growth in batch culture and analysis of metabolites in***
319 ***culture supernatants by GC-MS and LC-MS.*** To characterize the growth of *C.*
320 *sporogenes* with amino acids (**Extended data Fig. 1a**), cells were cultured in SACC
321 medium supplemented with 23 amino acids including the 20 proteinogenic amino acids
322 and L-citrulline, L-ornithine, and *trans*-4-hydroxyproline (1 mM each) and glucose (1
323 mM). Wild-type *C. sporogenes* was streaked from an anaerobic glycerol stock onto
324 RCM agar plates and incubated for ~24 h at 37 °C. Individual well-isolated colonies
325 were then inoculated into 5 mL of SACC (23 AA + glucose) medium and cultured for 24

326 h at 37 °C. Optical densities at 600 nm (OD600 nm) were recorded for cultures, then
327 cells were subcultured in 5 mL of SACC (23 AA + glucose) at a starting OD of 0.01 in
328 butyl rubber stoppered anaerobic Balch-type tubes (ChemGlass). Cultures were
329 incubated outside of the anaerobic chamber in a water bath set to 37 °C, and optical
330 density measurements were made hourly using a GENESYS 30 spectrophotometer
331 from Thermo Scientific. Samples (1 mL) were collected at 0 and 24 h, centrifuged at
332 5,000*g* for 10 min at 4 °C, then supernatants (500 μL) were collected and stored at -20
333 °C until analysis by GC-MS or LC-MS.

334 To characterize the growth phenotype of *rnfB* and *rnfE* mutants (**Fig. 4c**), cells
335 were cultured as above with the following minor modifications. The medium used was
336 SACC medium with 10 essential amino acids (1 mM each), with or without glucose (10
337 mM). Mutant cells were first streaked from anaerobic glycerol stocks onto RCM agar
338 plates with erythromycin (5 μg mL^{-1}), to confirm they carried the Clostron insertion, and
339 all subsequent growth was performed without supplemental antibiotics.

340 *Amino acid analysis in culture supernatants (corresponding to* ***Extended data***
341 ***Fig. 1b****).* Culture supernatant was diluted 80-fold with LC-MS grade water, then 50 μL of
342 samples or appropriately diluted standards (Sigma AAS18 supplemented with Trp, Asn,
343 Gln, ornithine, *trans*-4-hydroxyproline, and 5-aminovalerate) were combined with 10 μL
344 internal standards (L-Arginine:HCl (Guanido-$^{15}N_2$), DL-Valine (D8), L-Methionine
345 (Methyl-D3), L-Phenylalanine (D8), L-Leucine (D10), and L-Tyrosine (D7), 10 μM each)
346 in 96-well V-bottom plates from USA scientific. Then 25 μL of 0.1 M sodium tetraborate
347 and 50 μL of dansyl chloride (25 mM in 100% acetonitrile) were added. The solution

348 was mixed five times by pipetting, then incubated at room temperature in the dark for 15
349 min, mixed by pipetting five times, then incubated for an additional 15 min. The reaction
350 was quenched by the addition of 50 μL 0.5% formic acid, and the plate was centrifuged
351 at 5,000*g* for 15 min at room temperature. One hundred and twenty-five microliters were
352 then transferred to a Multiscreen Solvinert Filter Plate 0.45 μM (Millipore) placed on top
353 of a 96-well 0.5 mL polypropylene microplate (Agilent) which was then centrifuged at
354 5,000*g* for 5 min at room temperature. A cap mat was placed on the plate, and samples
355 were analyzed by LC-MS using an Agilent 1290 Infinity II UPLC equipped with a Waters
356 BEH C18 1.7-μm particle size C18 column (2.1 × 100 mm) and detected using an
357 Agilent 6545XT Q-TOF equipped with a dual jet stream electrospray ionization source
358 operating under extended dynamic range (EDR 1700 m/z) in positive ionization mode.
359 Eluent A consisted of 0.1% formic acid (v/v) in water and eluent B consisted of 0.1%
360 formic acid (v/v) in 100% acetonitrile. Five microliters of samples were injected via
361 refrigerated autosampler into mobile phase and chromatographic separation at 40 °C
362 was achieved at a flow rate of 0.5 mL min^{-1} using a linear gradient of 5–60% eluent B
363 over 10.25 min. Eluent B was brought to 95% over 2.25 min, held at 95% for 2.5 min,
364 brought to 5% over 0.1 min, and the column was then re-equilibrated at 5% eluent B for
365 2.9 min. Electrospray ionization parameters included a gas temperature of 325 °C,
366 drying gas flow of 10 L min^{-1}, nebulizer pressure of 20 psi, sheath gas temperature of
367 400 °C and flow of 12 L min^{-1}, and capillary voltage of 4000 V. MS1 spectra were
368 collected in profile mode, and peak assignments in samples were made based on
369 comparisons of retention times and accurate masses from authentic standards. Amino

370 acids were quantified by isotope-dilution mass spectrometry using L-Phenylalanine (D8)
371 as a suitable internal standard for most analytes.

372 *Aromatic fatty acids and amines by LC-MS (corresponding to* ***Extended data***
373 ***Fig. 1c, Extended data Fig. 6, Fig. 4d****).* Culture supernatants or appropriately diluted
374 standards (phenylacetate, phenylpropionate, 4-hydroxyphenylacetate, 3-(4-
375 hydroxyphenyl)propionate, indoleacetate, indolepropionate, tryptamine, 5-
376 aminovalerate) (100 μL) were combined with 450 μL of methanol followed by incubation
377 at room temperature for 5 min and centrifugation at 13,000*g* for 5 min at room
378 temperature. Subsequently, 200 μL of supernatant was transferred to wells of a 96-well
379 deep block plate and evaporated to dryness using a Biotage Turbovap. Then 200 μL of
380 resuspension solvent (0.1% formic acid (v/v) in water) containing internal standards
381 (100 μM *trans*-cinnamic acid (D7) and 50 μM indoleacetic acid (D5)) was added,
382 compounds were dissolved by vortexing for ~30 s and samples were clarified by
383 filtration through a Multiscreen Solvinert Filter Plate 0.45 μM (Millipore) placed on top of
384 a 96-well 0.5 mL polypropylene microplate (Agilent) by centrifugation at 5,000*g* for 5 min
385 at room temperature. A cap mat was placed on the plate, and samples were analyzed
386 by LC-MS using an Agilent 1290 Infinity II UPLC equipped with a Waters BEH C18 1.7-
387 μm particle size C18 column (2.1 × 100 mm) and detected using an Agilent 6545XT Q-
388 TOF equipped with a dual jet stream electrospray ionization source operating under
389 extended dynamic range (EDR 1700 m/z) in negative ionization mode. Eluent A
390 consisted of 6.5 mM ammonium bicarbonate in water and eluent B consisted of 6.5 mM
391 ammonium bicarbonate in 100% methanol. Five microliters of samples were injected via
392 refrigerated autosampler into mobile phase and chromatographic separation was

393 achieved at a flow rate of 0.35 mL min^{-1} using a linear gradient of 0.5–70% eluent B
394 over 4 min. Eluent B was brought to 98% over 0.5 min, held at 98% for 0.9 min, then
395 brought to 0.5% over 0.2 min and the column was re-equilibrated at 0.5% eluent B for
396 3.4 min. Peak assignments in samples were made based on comparisons of retention
397 times and accurate mass-to-charge ratios from authentic standards analyzed under
398 identical conditions. Electrospray ionization parameters included a gas temperature of
399 250 °C, drying gas flow of 6 L min^{-1}, nebulizer pressure of 30 psi, sheath gas
400 temperature of 200 °C and flow of 11 L min^{-1}, capillary voltage of 4000 V, and nozzle
401 voltage of 1400 V. MS1 spectra were collected in centroid mode, and peak assignments
402 in samples were made based on comparisons of retention times and accurate masses
403 from authentic standards. Aromatic fatty acids were quantified by isotope-dilution mass
404 spectrometry using *trans*-cinnamic acid (D7) or indoleacetic acid (D5) as internal
405 standards.

406 *Short chain fatty acids by GC-MS (corresponding to **Extended data Fig. 1c**).*
407 Culture supernatants (50 μL) were acidified with 6 M HCl (50 μL), then diluted in LC-MS
408 grade water (150 μL). Organic acids were then extracted with one volume of diethyl
409 ether (250 μL). An aliquot (95 μL) of the organic layer was transferred to a new sealed
410 vial, combined with *N-tert*-butyldimethylsilyl-*N*-methyltrifluoroacetamide (MTBSTFA, 5
411 μl) and derivatized at room temperature for 48 h. One microliter was then injected onto
412 an Agilent 7820A gas chromatograph equipped with an Agilent VF-5HT column (30 m x
413 0.25 mm x 0.1 μm) coupled to an Agilent 5977B mass spectrometer. The inlet was set
414 to 280 °C, and injection occurred in split mode with a ratio of 10:1. Oven conditions
415 were as follows: 50 °C for 2 min, ramped to 70 °C at 10 °C min^{-1}, then ramped to 85 °C

416 at 3 °C min^{-1}, then ramped to 290 °C at 30 °C min^{-1}. The mass spectrometer transfer
417 line was set to 250 °C, and the quadrupole was set at 150 °C. MS data was collected
418 under scan mode from 50 – 300 m/z with a 3 min solvent delay.

419 ***Wild-type C. sporogenes mono-colonization in gnotobiotic mice and***
420 ***analysis of metabolites in body fluids (corresponding to Fig. 1a,c, Supplementary***
421 ***Tables 1-4).*** Mouse experiments were performed on gnotobiotic Swiss Webster germ-
422 free mice originally obtained from Taconic Biosciences maintained in aseptic isolators.
423 Animal experiments were performed following a protocol approved by the Stanford
424 University Administrative Panel on Laboratory Animal Care. Mice (female, 9 weeks of
425 age, n = 5 per group, two groups) were colonized with wild-type *C. sporogenes* by oral
426 gavage (300 μL, ~1 × 10^8 CFU) and were maintained on standard chow (LabDiet 5k67).
427 After one week, group 1 mice were maintained on normal drinking water, while group 2
428 mice were switched to water containing antibiotics (0.5 mg/mL Vancomycin and 1
429 mg/mL Metronidazole) for another week before euthanization. Blood, urine and feces
430 were collected at 3 time points: before gavage with bacteria, 1 week and 2 weeks after
431 colonization. Cecal contents were harvested after euthanization. Blood collected from
432 the facial vein was mixed with EDTA (~15 mM EDTA, final) and centrifuged at 1,500*g*
433 for 15 min at 10 °C. Plasma was transferred to a new tube and stored at -80 °C until LC-
434 MS was performed. Fresh urine, fecal pellets, and cecal contents were collected and
435 stored at -80 °C until LC-MS was performed.

436 *Sample preparation for metabolite analysis in blood, urine, feces, and cecal*
437 *contents.* Mice urine samples (2.5 μL) were diluted with 7.5 μL LC-MS water. Blood (10

438 μL) and diluted urine (10 μL) samples were added to a 96-well V-bottom plate
439 containing internal standard mixture (tryptamine (D4), indoleacetic acid (D5),
440 phenylacetic acid (D5), phenylpropionic acid (D9), phenylalanine (D5), hippuric acid
441 (D2), 0.2 mM each, creatinine (D3), acetic acid ($^{13}C_2$), isovaleric acid (D2), 1 mM each,
442 10 μL) and 180 μL methanol. The solution was mixed five times by pipetting, then the
443 plate was centrifuged at 5,000*g* for 15 min at 4 °C. Supernatant was collected for the
444 following sample preparations, either derivatization or direct dilution, before subjecting
445 to LC-MS analysis.

446 Mice cecal contents and fecal samples (40(±4) mg) were weighed in
447 microcentrifuge tubes (Fisherbrand cat. # 02-682-558) containing glass beads (Sigma
448 cat. # G1145, 150-212 μm, 40(±4) mg). LC-MS water (40 μL), internal standard mixture
449 (tryptamine (D4), indoleacetic acid (D5), phenylacetic acid (D5), phenylpropionic acid
450 (D9), phenylalanine (D5), 0.2 mM, acetic acid ($^{13}C_2$) and isovaleric acid (D2), 1 mM
451 each, 80 μL), and methanol (1440 μL) were added to the tubes. The samples were
452 homogenized with a mixer mill (RETSCH MM400) at 4 °C, 25/s, for 30 min, then
453 centrifuged at 13,000*g* for 5 min at 4 °C. Supernatants were collected for the following
454 sample preparations, either derivatization or direct dilution, before subjecting to LC-MS
455 analysis.

456 *Derivatization method for short chain fatty acids.* Thirty microliters of supernatant
457 was transferred to a 96-well V-bottom plates and mixed with 15 μL 3-
458 nitrophenylhydrazine (200 mM in 50% acetonitrile) and 15 μL *N*-(3-
459 dimethylaminopropyl)-*N′*-ethylcarbodiimide (120 mM in 6% pyridine). The plates were

460 sealed with a plastic sealing mat (Thermo Fisher Scientific cat. # AB-0566) and
461 incubated at 40 °C, 900 rpm in a thermomixer for 30 min to derivatize the short chain
462 fatty acids. Eight microliters of the reaction mixture were quenched with 192 μL 0.02%
463 formic acid in 10% acetonitrile/water.

464 *Direct dilution method for other metabolites.* Thirty microliters of supernatant
465 were directly transferred to a 96-well V-bottom plates and diluted with LC-MS grade
466 water (90 μL) for LC-MS analysis.

467 *LC-MS conditions for detection and quantitation of metabolites.* The samples
468 were analyzed using the same instrument and column with the following methods.

469 (i) Derivatized acetate, propionate, butyrate, isobutyrate, 2-methylbutyrate, isovalerate,
470 isocaproate, 5-aminovaleric acid, indoleacetate, indolepropionate, phenylacetate,
471 phenylpropionate, 3-(4-hydroxyphenyl)acetate, 3-(4-hydroxyphenyl)propionate,
472 hippurate, phenylacetylglycine, phenylpropionylglycine, 4-hydroxyhippurate, (3-(4-
473 hydroxyphenyl)propanoyl)glycine, and 4-hydroxyphenylacetylglycine were analyzed
474 under negative ionization mode. Eluent A consisted of 0.1% formic acid (v/v) in water
475 and eluent B consisted of 0.1% formic acid (v/v) in 100% methanol. Samples (10 μL)
476 were injected via refrigerated autosampler into mobile phase and separation was
477 achieved with Waters BEH C18 1.7-μm particle size C18 columns (2.1 × 100 mm) at 50
478 °C using dual binary pumps with alternating column regeneration. The analytical pump
479 applied the following gradient at a flow rate of 0.3 mL min^{-1}: 0−11 min, 15% to 65% B,
480 11−11.1 min, 65% to 15% B, 11.1 min−12 min, 15% B. The regeneration pump applied
481 the following gradient at a flow rate of 0.2 mL min^{-1}: 0−0.1 min, 15% to 99.9% B, 0.1−6

482 min, 99.9% B, 6−9 min, 99.9% to 15% B, 9−12 min, 15% B. Electrospray ionization
483 parameters included a gas temperature of 300 °C, drying gas flow of 6 L min^{-1},
484 nebulizer pressure of 30 psi, sheath gas temperature of 300 °C and flow of 11 L min^{-1},
485 capillary voltage of 4000 V, and fragmentor voltage of 140 V.

486 (ii) Underivatized creatinine and tryptamine were analyzed under positive ionization
487 mode. Eluent A consisted of 0.1% formic acid (v/v) in water and eluent B consisted of
488 0.1% formic acid (v/v) in 100% methanol. Samples (0.5 μL) were injected via
489 refrigerated autosampler into mobile phase and separation was achieved with Waters
490 BEH C18 1.7-μm particle size C18 columns (2.1 × 100 mm) at 25 °C using dual binary
491 pumps with alternating column regeneration. The analytical pump applied the following
492 gradient at a flow rate of 0.3 mL min^{-1}: 0−4 min, 1% to 70% B, 4−4.01 min, 70% to 1%
493 B, 4.01−5 min, 1% B. The regeneration pump applied the following gradient at a flow
494 rate of 0.3 mL min^{-1}: 0−0.1 min, 1% to 98% B, 0.1−3 min, 98% B, 3−3.1 min, 98% to 1%
495 B, 3.1−5 min, 1% B. Electrospray ionization parameters included a gas temperature of
496 250 °C, drying gas flow of 6 L min^{-1}, nebulizer pressure of 30 psi, sheath gas
497 temperature of 250 °C and flow of 11 L min^{-1}, capillary voltage of 4000 V, and
498 fragmentor voltage of 70 V.

499 Selection of internal standards (ISTD) for LC-MS quantitation were as follows:
500 isovaleric acid (D2) as ISTD for butyrate, isobutyrate, 2-methylbutyrate, isovalerate, and
501 isocaproate. Indoleacetic acid (D5) as ISTD for indoleacetate, indolepropionate, 4-
502 hydroxyhippurate, (3-(4-hydroxyphenyl)propanoyl)glycine, and 4-
503 hydroxyphenylacetylglycine. Phenylacetic acid (D5) as ISTD for phenylacetate.
504 Phenylpropionic acid (D9) as ISTD for phenylpropionate, 4-OH-phenylpropionate, 4-OH-

505 phenylacetate, and phenylacetylglycine. Acetic acid ($^{13}C_2$) as ISTD for acetate,
506 propionate, and 5-aminovaleric acid. Tryptamine (D4) as ISTD for tryptamine. Hippurate
507 (D2) as ISTD for hippurate.

508 ***Analysis of metabolites in human plasma (corresponding to Fig. 1d,***
509 ***Supplementary Table 5).*** De-identified human plasma samples were obtained from the
510 Stanford Blood Center under their IRB-approved research protocol. Thawed samples
511 were mixed by gentle inversion and aliquots (50 μL) were transferred to a 96-well V-
512 bottom plate containing internal standard mixture (tryptamine (D4), indoleacetic acid
513 (D5), phenylacetic acid (D5), phenylpropionic acid (D9), phenylalanine (D5), hippuric
514 acid (D2), acetic acid ($^{13}C_2$), isovaleric acid (D2), 40 μM each, 5 μL) and acetonitrile:
515 methanol 3:1 mixture (150 μL). The solution was mixed five times by pipetting, then the
516 plate was centrifuged at 5,000*g* for 15 min at 4 °C. Supernatant was collected for the
517 following sample preparations, either derivatization or direct dilution, before being
518 subjected to LC-MS analysis. Derivatization was performed as the protocol described
519 above with the following minor adjustment: after reaction completion, sixteen microliters
520 of the reaction mixture were quenched with 184 μL 0.04% formic acid in 10%
521 acetonitrile/water. Direct dilution was performed as described above, but with the
522 following minor adjustment: seventy microliters of supernatant were directly transferred
523 to a 96-well V-bottom plates and diluted with LC-MS grade water (70 μL) for LC-MS
524 analysis.

525 Derivatized acetate, propionate, butyrate, isobutyrate, 2-methylbutyrate,
526 isovalerate, isocaproate, 5-aminovalerate, indoleacetate, indolepropionate,
527 phenylacetate, phenylpropionate, 3-(4-hydroxyphenyl)acetate, 3-(4-

528 hydroxyphenyl)propionate, hippurate, phenylacetylglycine, phenylpropionylglycine, 4-
529 hydroxyhippurate, (3-(4-hydroxyphenyl)propanoyl)glycine, and 4-
530 hydroxyphenylacetylglycine were analyzed with the same acquisition method as
531 described above for mouse plasma samples, except that 20 μL of samples were
532 injected.

533 ***Stable isotope amino acid conversion in culture and in cell suspensions***
534 ***(corresponding to Fig. 2b,d, Extended data Fig. 4 and 5).*** To monitor consumption of
535 specific amino acids during growth, we prepared SACC medium containing all 20
536 proteinogenic amino acids and glucose (10 mM), where individual amino acids (Val, Ile,
537 Leu, Pro, Phe, Tyr, Trp) were substituted their deuterium labeled isotopologues (Val
538 (D8), Ile (D10), Leu (D10), Pro (D7), Phe (D8), Tyr (D4), Trp (D5)). Wild-type *C.*
539 *sporogenes* were streaked from an anaerobic glycerol stock onto RCM agar plates, and
540 incubated for ~20 h at 37 °C. Individual well-isolated colonies were inoculated into 4 mL
541 of SACC containing 20 AA (1 mM each) and glucose (10 mM) and cells were cultured
542 for 20 h at 37 °C. Cells were diluted to ~0.01 OD_{600nm} into fresh SACC with 19 unlabeled
543 amino acid plus one stable isotope labeled amino acid (1 mM each) and glucose (10
544 mM) and cultured for 24 h at 37 °C. At 0 h, 6 h, and 24 h, 200 μL aliquots of culture was
545 transferred to pre-chilled tubes and was centrifuged at ~13,000*g* speed for 1 min at 4
546 °C. Supernatant was transferred to a new tube and stored at -80 °C until LC-MS
547 measurement.

548 *C. sporogenes* requires 10 essential amino acids to support its growth,
549 complicating analysis of its metabolism. To avoid interference from other amino acids,
550 we used whole cell suspensions to measure single or paired amino acid conversions.

551 Individual well-isolated colonies of *C. sporogenes* were inoculated into 4 mL of SACC
552 broth plus 1 mM *trans*-4-hydroxy-L-proline and were cultured for 14 h at 37 °C.
553 Overnight cultures were diluted to ~0.01 OD_{600nm} into the same medium and incubated
554 for 4 h at 37 °C until 0.15 ~0.2 OD_{600nm}. Cells were spin down anaerobically at 6,500*g*
555 for 8 min at room temperature. Cell pellet was washed by SACC-basal solution (no
556 amino acid nor carbon source) and resuspended in the same solution. Cell suspension
557 was mixed with designed amino acid(s) (final 5 mM amino acid and OD_{600nm} =1 of cells
558 if not specified) and incubate at 37 °C anaerobic incubator. For Val and Pro pair, 5 mM
559 Val and 10 mM Pro were used to match stoichiometric requirements[15]. At T=0, 30 min,
560 60 min, and 180 min, assay aliquots (200 μL) were transferred to pre-chilled Eppendorf
561 tubes. After centrifugation at ~13,000*g* for 1 min at 4 °C, supernatant (120 μL) was
562 transferred to a new tube and stored at -80 °C until LC-MS measurements.

563 *Stable isotope-labeled amino acid and metabolite analysis by LC-MS for stable*
564 *isotope amino acid conversion in growth culture and in whole cell suspension (Val, Pro)*.
565 Culture supernatants (10 μL) were mixed with internal standards (phenylethylamine
566 (D5), phenylpropionic acid (D9), phenylalanine (D5), alanine (D4) and isovaleric acid
567 (D2), 5 mM each, 10 μL) and diluted with LC-MS grade water (30 μL) in 96-well V-
568 bottom plates (USA scientific cat. # 1833-9600). Then 150 μL of acetonitrile/methanol
569 (3:1 ratio) was added. The solution was mixed five times by pipetting, then the plate was
570 centrifuged at 5,000*g* for 10 min at 4 °C. Supernatant was collected for the following
571 sample preparations, either derivatization or direct dilution, before subjecting to LC-MS
572 analysis.

573 Derivatization for short chain fatty acid was performed as the protocol described
574 above with slight modification: after derivatization, 2 μL of the reaction mixture were
575 then quenched in a new 96-well V-bottom plate containing 0.02% formic acid in 10%
576 acetonitrile/water (98 μL) and subjected to LC-MS analysis.

577 Direct dilution method: five microliters of supernatant were directly transferred to
578 a 96-well V-bottom plates and diluted with LC-MS grade water (95 μL) for LC-MS
579 analysis.

580 The samples were analyzed using an Agilent 6545XT Q-TOF mass spectrometer
581 equipped with a dual jet stream electrospray ionization source operating under
582 extended dynamic range (EDR 1700 m/z). Reverse phase separation was performed on
583 an Agilent 1290 Infinity II LC system equipped with Waters BEH C18 1.7-μm particle
584 size columns (2.1 × 100 mm) for all reversed phase (RP) separation.

585 Derivatized short chain fatty acids (acetate (D2 and D3), propionate (D3 and D5),
586 isobutyrate (D7), butyrate (D7), 2-methyl-butyrate (D9), isovalerate (D9), isocaproate
587 (D9 and D10)) were analyzed under negative ionization mode. Eluent A consisted of
588 0.1% formic acid (v/v) in water and eluent B consisted of 0.1% formic acid (v/v) in 100%
589 acetonitrile. Samples (2 μL) were injected via refrigerated autosampler into mobile
590 phase and separation was achieved at 40 °C using dual binary pumps with alternating
591 column regeneration. The analytical pump applied the following gradient at a flow rate of
592 0.4 mL min^{-1}: 0−3 min, 15% B, 3−10 min, 15% to 40% B, 10−10.1 min, 40% to 15% B,
593 10.1 min−11 min, 15% B. The regeneration pump applied the following gradient at a
594 flow rate of 0.2 mL min^{-1}: 0−7 min, 98% B, 7−8 min, 98% to 15% B, 8−11 min, 15% B.

595 Electrospray ionization parameters included a gas temperature of 300 °C, drying gas
596 flow of 6 L min^{-1}, nebulizer pressure of 30 psi, sheath gas temperature of 300 °C and
597 flow of 11 L min^{-1}, capillary voltage of 4000 V, and fragmentor voltage of 140 V.

598 Underivatized arginine (D7), serine (D3), *trans*-4-hydroxyproline (D3 and D6),
599 proline (D7), 5-aminovalerate (D2 and D6), valine (D8), isoleucine (D10), tyrosine (D4),
600 leucine (D10), phenylalanine (D8), tryptamine (D5), and tryptophan (D5) were analyzed
601 under positive ionization mode. Eluent A consisted of 0.2% formic acid (v/v) in water
602 and eluent B consisted of 0.2% formic acid (v/v) in 100% methanol. Samples (0.5 μL)
603 were injected via refrigerated autosampler into mobile phase and separation at 25 °C
604 was achieved at a flow rate of 0.2 mL min^{-1} using the following gradient: 0−3 min, 1% B,
605 3−5 min, 1% to 98% B, 5−7 min, 98% B, 7−7.01 min, 98% to 1% B, 7.01−9.7 min, 1%
606 B. Electrospray ionization parameters included a gas temperature of 300 °C, drying gas
607 flow of 6 L min^{-1}, nebulizer pressure of 30 psi, sheath gas temperature of 275 °C and
608 flow of 11 L min^{-1}, capillary voltage of 4000 V, and fragmentor voltage of 140 V.

609 Underivatized aromatic metabolites (4-OH-phenylpropionate (D4), 4-OH-
610 phenylacetate (D4), indolepropionate (D5), indoleacetate (D5), phenylpropionate (D6),
611 phenylacetate (D7)) were analyzed under negative ionization mode. Eluent A consisted
612 of 0.1% acetic acid (v/v) in water and eluent B consisted of 0.1% acetic acid (v/v) in
613 100% acetonitrile. Samples (0.5 μL) were injected via refrigerated autosampler into
614 mobile phase and separation at 40 °C was achieved at a flow rate of 0.3 mL min^{-1} using
615 the following gradient: 0−4 min, 10% to 60% B, 4−4.5 min, 60% to 98% B, 4.5−6 min,
616 98% B, 6−6.01 min, 98% to 10% B, 6.01−9 min, 10% B. Electrospray ionization

617 parameters included a gas temperature of 300 °C, drying gas flow of 6 L min^{-1},
618 nebulizer pressure of 30 psi, sheath gas temperature of 275 °C and flow of 11 L min^{-1},
619 capillary voltage of 4000 V, and fragmentor voltage of 140 V.

620 MS1 spectra were collected in centroid mode, and peak assignments in samples
621 were made based on comparisons of retention times and accurate masses from
622 unlabeled standards. Amino acids and metabolites were quantified by isotope-dilution
623 mass spectrometry using corresponding ISTD. Selection of internal standards for LC-
624 MS quantitation are as follows: phenylalanine (D5) as ISTD for arginine (D7), valine
625 (D8), isoleucine (D10), tyrosine (D4), leucine (D10), phenylalanine (D8), tryptamine
626 (D5), and tryptophan (D5). Alanine (D4) as ISTD for 5-aminovalerate (D2 and D6),
627 *trans*-4-hydroxyproline (D3 and D6), proline (D7), and serine (D3). Phenylethylamine
628 (D5) as ISTD for tryptamine (D5). Phenylpropionic acid (D9) as ISTD for 4-OH-
629 phenylpropionate (D4), 4-OH-phenylacetate (D4), indolepropionate (D5), indoleacetate
630 (D5), phenylpropionate (D6), and phenylacetate (D7). Isovaleric acid (D2) as ISTD for
631 short chain fatty acids.

632 *Analysis of stable isotope-labeled amino acids and metabolites in whole cells*
633 *suspension (Phe, Trp, Tyr).* Culture supernatants (10 μL) were prepared using the
634 above method with slight changes. 1) The concentration of internal standards changed
635 as follows: phenylethylamine (D5), phenylpropionic acid (D9), phenylalanine (D5),
636 alanine (D4), 0.2 mM each, and isovaleric acid (D2), 1 mM). 2) Aromatic amino acid
637 metabolites (4-OH-phenylpropionate (D4), 4-OH-phenylacetate (D4), indolepropionate
638 (D5), indoleacetate (D5), phenylpropionate (D6), and phenylacetate (D7)) were
639 derivatized using the same method and analyzed together with short chain fatty acids.

640 No separate analysis of underivatized metabolites under negative ionization mode was
641 performed. Eluent A consisted of 0.1% acetic acid (v/v) in water and eluent B consisted
642 of 0.1% acetic acid (v/v) in 100% acetonitrile. Samples (1 μL) were injected via
643 refrigerated autosampler into mobile phase and separation was achieved with Waters
644 BEH C18 1.7-μm particle size C18 columns (2.1 × 100 mm) at 40 °C using dual binary
645 pumps with alternating column regeneration. The analytical pump applied the following
646 gradient at a flow rate of 0.4 mL min^{-1}: 0−4 min, 3% to 50% B, 4−4.1 min, 50% to 3% B,
647 4.1−5 min, 3% B. The regeneration pump applied the following gradient at a flow rate of
648 0.4 mL min^{-1}: 0−0.1 min, 3% to 98% B, 0.1−2 min, 98% B, 2−2.2 min, 98% to 3% B,
649 2.2−5 min, 3% B. Electrospray ionization parameters included a gas temperature of 250
650 °C, drying gas flow of 6 L min^{-1}, nebulizer pressure of 30 psi, sheath gas temperature of
651 250 °C and flow of 11 L min^{-1}, capillary voltage of 4000 V, and fragmentor voltage of 70
652 V.

653 Selection of internal standards for LC-MS quantitation was as follows:
654 phenylalanine (D5) as ISTD for arginine (D7), valine (D8), isoleucine (D10), tyrosine
655 (D4), leucine (D10), methionine (D8), phenylalanine (D8), tryptamine (D5), and
656 tryptophan (D5). Alanine (D4) as ISTD for 5-aminovalerate (D2 and D6), *trans*-4-
657 hydroxyproline (D3 and D6), proline (D7), and serine (D3). Phenylethylamine (D5) as
658 ISTD for tryptamine (D5). Phenylpropionic acid (D9) as ISTD for 4-OH-phenylpropionate
659 (D4), 4-OH-phenylacetate (D4), indolepropionate (D5), indoleacetate (D5),
660 phenylpropionate (D6), and phenylacetate (D7). Isovaleric acid (D2) as ISTD for short
661 chain fatty acids.

662 ***ATP measurements in whole cells and detection of metabolites***

663 ***(corresponding to Fig. 3d, Extended data Fig. 6 and 7).*** Wild type *C. sporogenes*

664 cells were streaked from an anaerobic glycerol stock onto a TYG (3% w/v tryptone, 2%

665 w/v yeast extract, 0.1% w/v sodium thioglycolate) agar plate and incubated at 37 °C in

666 an anaerobic chamber from Coy Laboratories under an atmosphere of 5% H_2, 10% CO_2

667 and 85% N_2. After ~24 h, a well isolated colony was inoculated into 5 mL of TYG broth

668 and cultured to stationary phase (~24 h). Cells were diluted into 20 mL of TYG broth

669 (1000-fold dilution) and grown to late-log phase of growth (~16 h). The cells were then

670 harvested by centrifugation (5,000*g*, 10 min, 4 °C) and washed twice with 20 mL

671 volumes of pre-reduced phosphate assay buffer (40 mM potassium phosphate, 10 mM

672 magnesium sulfate, pH 7.0). All centrifugation steps were performed outside of the

673 anaerobic chamber, and so to ensure anaerobiosis, 50 mL falcon tubes were tightly

674 capped and care was taken to limit the total amount of time outside of the chamber.

675 After the final wash step, the cell pellet was re-suspended in 1 ml of phosphate assay

676 buffer and incubated at room temperature for 45 min to achieve a resting cell

677 suspension. During this time, 100 μL of cells were seeded into rows of a 96-well

678 microtiter plate (12 wells per condition being tested). Two hundred microliters of pre-

679 reduced 2 mM substrate in phosphate assay buffer, or buffer alone was dispensed into

680 rows of a separate 96-well microplate. At time zero, 100 μL of substrate or buffer was

681 added to the cells and mixed gently by pipetting. At - 5 min, - 1 min, +30 s, +1 min, +2

682 min, +5 min, +10 min, +20 min, +30 min, +45 min, +60 min, and +90 min, 10 μL of cells

683 were taken and immediately mixed with 90 μL of DMSO to quench the reaction and

684 liberate cellular ATP. The -5 and -1 minute time-points were taken prior to addition of

685 buffer or substrate, so only 5 μL of cell suspension was harvested, and 5 μL of either
686 buffer or substrate was added to the cell-DMSO mixtures to bring the total volume to
687 100 μL. At the end of the assay, a 50 μL aliquot of cell suspension was taken for
688 subsequent total protein determination. The ATP content from 10 μL aliquots of lysed
689 cells was then detected using a luminescence-based ATP determination kit from Life
690 Technologies and ATP levels were calculated by extrapolation from a calibration curve
691 constructed with known concentrations of ATP. For protein determination, cellular
692 protein was solubilized in NaOH by combining equal volumes of cells and 0.4 M NaOH
693 (50 μL, each) and incubating at 99 °C for 10 minutes. The protein content was then
694 determined using the DC Protein Assay Kit II from BioRad using bovine serum albumin
695 as a standard. ATP levels were expressed as nmol of ATP per mg of total protein.

696 To test the effect of 3,3',4',5-tetrachlorosalicylanilide (TCS) on ATP formation,
697 washed cells first were rested at room temperature anaerobically for 30 min. Then TCS
698 (diluted from a 100 X stock in ethanol to achieve the desired concentration) was added
699 and cells were incubated at room temperature for an additional 30 min. Assays were
700 then performed as described above, and ten microliters of DMSO quenched samples
701 were used immediately for ATP measurement, with the remaining 90 μL being stored at
702 -80 °C until LC-MS measurements.

703 Before LC-MS measurement, DMSO quenched samples (90 μL) were thawed at
704 room temperature and then centrifuged at 5,000*g* for 15 min at room temperature.

705 For quantitation of phenylalanine, phenylethylamine, phenyllactate,
706 phenylpyruvate, trans-cinnamate, PPA, PPG, and PAA, supernatant (60 μL) was mixed

707 with internal standard solution (PPA (D9), phenylalanine (D5), phenylethylamine (D5),
708 PAA (D5), 100 μM each, 6 μL). Twenty-five microliters of the above mixture were diluted
709 with 75 μL LC-MS grade water. Eluent A consisted of 0.1% acetic acid (v/v) in water and
710 eluent B consisted of 0.1% acetic acid (v/v) in 100% acetonitrile. Samples (1 μL) were
711 injected via refrigerated autosampler into mobile phase and separation with a BEH C18
712 1.7-μm particle size C18 column (2.1 × 100 mm) at 40 °C was achieved at a flow rate of
713 0.4 mL min^{-1} with the following gradient: 0−1 min, 3% B, 1−4 min, 3% to 60% B, 4−4.1
714 min, 60% to 99.9% B, 4.1−7 min, 99.9% B, 7−7.1 min, 99.9% to 3% B, 7.1−9 min, 3% B.
715 Two-time segments were applied for mass spectra acquisition. Segment 1 from 0.5 to
716 2.65 min was set under positive ionization mode for analysis of phenylalanine and
717 phenylethylamine. Segment 2 from 2.65 to 5 min was set under negative ionization
718 mode for analysis of other metabolites. Electrospray ionization parameters included a
719 gas temperature of 250 °C, drying gas flow of 6 L min^{-1}, nebulizer pressure of 30 psi,
720 sheath gas temperature of 250 °C and flow of 11 L min^{-1}, capillary voltage of 4000 V,
721 and fragmentor voltage of 70 V.

722 For quantitation of proline and 5-aminovalerate, supernatant (60 μL) was mixed
723 with internal standard (phenylalanine (D5), 100 μM, 6 μL). Twenty-five microliters were
724 diluted with 50% acetonitrile containing 0.1% acetic acid (75 μL) for quantitation of
725 proline and 5-aminovalerate. The analytes were measured with hydrophilic interaction
726 liquid chromatography (HILIC) using a Waters BEH amide 1.7-μm particle size column
727 (2.1 × 100 mm). Eluent A consisted of 5 mM ammonium acetate, 0.1% acetic acid (v/v)
728 in water, and eluent B consisted of 5 mM ammonium acetate, 0.1% acetic acid (v/v) in
729 90% acetonitrile. Samples (2 μL) were injected via refrigerated autosampler into mobile

730 phase and HILIC separation at 50 °C was achieved at a flow rate of 0.4 mL min^{-1} with
731 the following gradient: 0−1 min, 80% B, 1−2.5 min, 80% to 40% B, 2.5−3.5 min, 40% B,
732 3.5−4 min, 40% to 80% B, 4−7 min, 80% B. Mass spectra were acquired under negative
733 ionization mode with the following parameters: gas temperature of 250 °C, drying gas
734 flow of 6 L min^{-1}, nebulizer pressure of 30 psi, sheath gas temperature of 250 °C and
735 flow of 11 L min^{-1}, capillary voltage of 4000 V, and fragmentor voltage of 70 V.

736 MS1 spectra were collected in centroid mode, and peak assignments in samples
737 were made based on comparisons of retention times and accurate masses from
738 standards. Amino acids and metabolites were quantified by isotope-dilution mass
739 spectrometry using corresponding ISTD. Selection of internal standards for LC-MS
740 quantitation are as follows: phenylalanine (D5) as ISTD for arginine (D7), valine (D8),
741 isoleucine (D10), tyrosine (D4), leucine (D10), phenylalanine (D8), tryptamine (D5), and
742 tryptophan (D5).

743 ***Colonization of gnotobiotic mice with wild-type or rnfB mutant C.***
744 ***sporogenes and analysis of indolepropionate in cecal contents and serum***
745 ***(corresponding to Fig. 4e).*** Mouse experiments were performed on gnotobiotic Swiss
746 Webster germ-free mice (male, 6–10 weeks of age, n = 5 per group) originally obtained
747 from Taconic Biosciences maintained in aseptic isolators. Animal experiments were
748 performed following a protocol approved by the Stanford University Administrative Panel
749 on Laboratory Animal Care. Separate groups of mice were colonized with wild-type or
750 *rnfB* mutant *C. sporogenes* by oral gavage (200 μL, ~1 × 10^7 CFU) and housed in
751 separate flexible film isolators. After 2 weeks, mice were euthanized and blood was
752 collected by cardiac puncture, placed in serum separator tubes (BD cat. # 365967),

753 mixed briefly, incubated at room temperature for ~30 min, then serum was obtained by
754 centrifuging tubes at 10,000*g* for 10 min at room temperature. Cecal contents were also
755 collected and along with serum aliquots were stored at -80 °C until analysis.
756 Indolepropionate was then quantified by LC-MS as described in the section above for
757 metabolite analysis in body fluids of gnotobiotic mice.

758 ***Competition experiments for wild-type and rnfB mutant C. sporogenes in***
759 ***gnotobiotic mice.*** Mouse experiments were performed on gnotobiotic Swiss Webster
760 germ-free mice (male, 6–10 weeks of age, n = 5 per group) originally obtained from
761 Taconic Biosciences maintained in aseptic isolators. Animal experiments were
762 performed following a protocol approved by the Stanford University Administrative Panel
763 on Laboratory Animal Care. For the mono-colonization experiments, mice were
764 colonized with a 1:1 mixture of wild-type and *rnfB* mutant *C. sporogenes* by oral gavage
765 (200 μL, ~1 × 10^7 CFU) and were maintained on standard chow (LabDiet 5k67). For the
766 defined community, mice were first colonized with a mixture consisting of equal volumes
767 from cultures of *Bacteroides thetaiotaomicron* (~16 h overnight culture), *Bacteroides*
768 *vulgatus* (~ 16 h overnight culture), *Edwardsiella tarda* (~ 16 h overnight culture),
769 *Eubacterium rectale* (~24 h overnight culture), *Clostridium scindens* (~30 h culture), and
770 *Bifidobacterium breve* (~24 h overnight culture). After one week, mice were colonized
771 with a 1:1 mixture of wild--type or *rnfB* mutant *C. sporogenes* (200 μL, ~1 × 10^7 CFU)
772 and were maintained on standard chow (LabDiet 5k67). Fresh fecal pellets were
773 collected and stored at -80 °C until DNA extraction was performed.

774 *DNA isolation and Q-PCR.* Relative abundances of the wild-type and *rnfB C.*
775 *sporogenes* strains over time following colonization was determined by Q-PCR

776 (*corresponding to* ***Fig. 4f,g***). Approximately 10-20 mg of feces was added to individual
777 tubes of a DNeasy PowerSoil DNA Isolation Kit (formerly MO BIO) and DNA was
778 extracted using a Retsch MM400 ball mill according to manufacturer's guidelines. DNA
779 quantitation was performed with an Invitrogen Quant-iT broad range dsDNA assay kit.
780 Two primer sets were used, one designed to amplify total *C. sporogenes*, and another
781 specifically targeted to the erythromycin resistance cassette of the *rnfB* mutant
782 (**Supplementary Table 8**). To amplify genomic DNA (gDNA), we used the Brilliant III
783 SYBR kit from Agilent Technologies. Conditions were as follows: 96-well Q-PCR plates,
784 20 μL reactions, primers at 500 nM each, reference dye included, 5 ng DNA per
785 reaction. Amplification was performed in duplicate using a Stratagene Mx3000P with
786 PCR conditions supplied in the Brilliant III SYBR kit. Initial validation plots were
787 performed using eight serial 4-fold dilutions of gDNA from either WT or *rnfB* mutant *C.*
788 *sporogenes* spanning 50 ng to 3 pg per reaction. The cycle threshold vs. log(input DNA)
789 was plotted and a linear curve fit was applied. Both primers displayed excellent linearity
790 across this range of DNA concentrations (R^2>0.98). For fecal DNA samples, the cycle
791 number at the threshold crossing point was used to calculate the amount of total *C.*
792 *sporogenes* DNA or *rnfB* mutant DNA using the standard curves. The competitive index
793 was calculated according to equation 1 below:

794 eq (1) $$CI = \frac{(rnfB\ DNA)}{(Total\ DNA - rnfB\ DNA)}$$

795 Relative compositions of community members (*corresponding to* ***Extended data***
796 ***Fig. 10***) were measured by Q-PCR using PowerUp SYBR Green Master Mix (Thermo
797 Fisher, A25742), 400 nM primers, 5~15 ng DNA per reaction in 384-well Q-PCR plates

798 (Applied Biosystems™ Cat. # 4483285) with total 12 μL reaction. Amplification was
799 performed in triplicate using QuantStudio™ 5 according to SYBR Green user manual
800 following by melting curve. Primer validation were performed using six serial 10-fold
801 dilutions of gDNA from each strain, spanning 24 ng to 0.24 pg per reaction. Primer
802 amplification efficiency were between 92~100%. For fecal DNA samples, the amount of
803 each strains was calculated using the standard curves. The relative composition was
804 calculated according to equation 2 below:

805 eq (2) $$Relative\ composition\ of\ Strain\ 1\ (\%) = \frac{(Strain\ 1\ \ DNA)}{(Total\ DNA)} * 100\%$$

806

807 ***Bioinformatics analysis (corresponding to Extended data Fig. 11, 12 and***
808 ***Supplementary Table 6).***

809 *Analysis of Rnf clusters in reference genomes from the human microbiome project.*
810 Reference genomes (GenBank file format) from the NIH Human Microbiome Project
811 (BioProject ID 43021) were downloaded on June 19th, 2019 which included 2,284
812 genome sequences. We then used the software tool MultiGeneBlast[30] to search these
813 reference genomes for homologs of the *C. sporogenes* Rnf gene cluster (*rnfCDGEAB*,
814 CLOSPO_00568 to CLOSPO_00573) with default settings. The results were manually
815 curated to identify organisms harboring complete gene clusters. Coding sequences for
816 the 16S rRNA genes were retrieved for these organisms from the Joint Genome
817 Institute Integrated Microbial Genomes server. Sequences were uploaded into
818 Geneious Prime (v2019.1.3) and were aligned using MUSCLE with default settings.
819 Alignments were trimmed to remove incomplete sequences (<500 bp) and gaps, then

820 were re-aligned and a phylogenetic tree was constructed using the neighbor joining
821 method. Representative gene clusters were exported from MultiGeneBlast and
822 visualized in Adobe Illustrator (v25.1).

823 *Analysis of electron transfer proteins in GenBank.* To identify homologs of the
824 electron transfer proteins analyzed in this study, we performed BLASTp searches of the
825 GenBank database. Query sequences included the butyryl-CoA dehydrogenase (Bcd)
826 from *C. kluyveri* DSM 555 (GenBank acc. # EDK32509.1), the (aryl)acryloyl-CoA
827 dehydrogenase (AcdA) from *C. sporogenes* ATCC 15579 (GenBank acc. #
828 EDU39257.1), the isocaprenoyl-CoA dehydrogenase (AcdB) from *C. sporogenes* ATCC
829 15579 (GenBank acc. # EDU36591.1), the proline reductase subunit A (PrdA) from *C.*
830 *sticklandii* DSM 519 (GenBank acc. # CBH22353.1), and the RnfB protein from *C.*
831 *sporogenes* ATCC 15579 (GenBank acc. # EDU37753.1). Our initial analysis of gene
832 cluster neighborhoods for these homologs using MultiGeneBlast suggested a cutoff of
833 65% amino acid identify was necessary to identify likely isofunctional homologs for Bcd,
834 AcdA, AcdB, and PrdA, whereas a less stringent cutoff of 50% amino acid identity was
835 suitable for RnfB. These query sequences were used in BLASTp searches of the
836 GenBank database (December 30th, 2020) and homologs with less than 80% coverage
837 over the length of the proteins were discarded.

838 *Analysis of abundance and prevalence of electron transfer proteins in metagenomics*
839 *datasets.* To assess the abundance and prevalence of electron transfer proteins (Bcd,
840 AcdA, AcdB, PrdA, and RnfB) in human fecal metagenomic datasets, we employed the
841 web-based tool, MetaQuery[31]. Query sequences included the butyryl-CoA
842 dehydrogenase (Bcd) from *C. kluyveri* DSM 555 (GenBank acc. # EDK32509.1), the

843 (aryl)acryloyl-CoA dehydrogenase (AcdA) from *C. sporogenes* ATCC 15579 (GenBank
844 acc. # EDU39257.1), the isocaprenoyl-CoA dehydrogenase (AcdB) from *C. sporogenes*
845 ATCC 15579 (GenBank acc. # EDU36591.1), the proline reductase subunit A (PrdA)
846 from *C. sticklandii* DSM 519 (GenBank acc. # CBH22353.1), and the RnfB protein from
847 *C. sporogenes* ATCC 15579 (GenBank acc. # EDU37753.1). Owing to limitations in
848 threshold selections implemented in MetaQuery, we used a slightly lower threshold for
849 amino acid percent identity of 60% for Bcd, AcdA, AcdB, and PrdA to identify homologs
850 in metagenomics datasets.

851 **Data availability.** The authors declare that the data supporting the findings of this study
852 are available within the paper and its Supplementary Information.

853 **Acknowledgements**

854 We are grateful to Michael Fischbach, Christopher Walsh, Audrey Southwick and Curt
855 Fischer (Stanford) and Isaac Cann (Illinois) for valuable discussions. We thank
856 Manhong Wu for assistance with amino acid analysis by LC-MS, Michelle St. Onge with
857 help constructing mutants, and Chun-Jun Guo and Ricardo De La Pena for assistance
858 with GC-MS analysis of short chain fatty acids. This work was funded in part by National
859 Institutes of Health grants DK110335 (D.D.), DK101674 (J.L.S.), DK085025 (J.L.S.) and
860 the Chan Zuckerberg Biohub (J.L.S.).

861 **References**

862 1 Nisman, B. The Stickland reaction. *Bacteriol Rev* **18**, 16-42 (1954).
863 2 Smith, E. A. & Macfarlane, G. T. Dissimilatory amino acid metabolism in human colonic
864 bacteria. *Anaerobe* **3**, 327-337 (1997).
865 3 Russell, W. R. *et al.* Major phenylpropanoid-derived metabolites in the human gut can
866 arise from microbial fermentation of protein. *Mol Nutr Food Res* **57**, 523-535 (2013).
867 4 Van Treuren, W. & Dodd, D. Microbial contribution to the human metabolome:
868 Implications for health and disease. *Annu Rev Pathol* (2019).
869 5 Liu, Y., Hou, Y., Wang, G., Zheng, X. & Hao, H. Gut microbial metabolites of aromatic
870 amino acids as signals in host-microbe interplay. *Trends Endocrinol Metab* **31**, 818-834,
871 doi:10.1016/j.tem.2020.02.012 (2020).
872 6 Dodd, D. *et al.* A gut bacterial pathway metabolizes aromatic amino acids into nine
873 circulating metabolites. *Nature* **551**, 648-652 (2017).
874 7 Venkatesh, M. *et al.* Symbiotic bacterial metabolites regulate gastrointestinal barrier
875 function via the xenobiotic sensor PXR and Toll-like receptor 4. *Immunity* **41**, 296-310,
876 doi:10.1016/j.immuni.2014.06.014 (2014).
877 8 Roager, H. M. & Licht, T. R. Microbial tryptophan catabolites in health and disease. *Nat*
878 *Commun* **9**, 3294, doi:10.1038/s41467-018-05470-4 (2018).
879 9 Steed, A. L. *et al.* The microbial metabolite desaminotyrosine protects from influenza
880 through type I interferon. *Science* **357**, 498-502, doi:10.1126/science.aam5336 (2017).
881 10 Allison, M. J., Bryant, M. P. & Doetsch, R. N. Volatile fatty acid growth factor for
882 cellulolytic cocci of bovine rumen. *Science* **128**, 474-475 (1958).
883 11 Stack, R. J., Hungate, R. E. & Opsahl, W. P. Phenylacetic acid stimulation of cellulose
884 digestion by *Ruminococcus albus* 8. *Appl Environ Microbiol* **46**, 539-544 (1983).

885 12 Hungate, R. E. & Stack, R. J. Phenylpropanoic acid: Growth factor for *Ruminococcus*
886 *albus*. *Appl Environ Microbiol* **44**, 79-83 (1982).
887 13 Stickland, L. H. Studies in the metabolism of the strict anaerobes (genus *Clostridium*):
888 The chemical reactions by which *Cl. sporogenes* obtains its energy. *Biochem J* **28**,
889 1746-1759 (1934).
890 14 Barker, H. A. Amino acid degradation by anaerobic bacteria. *Annu Rev Biochem* **50**, 23-
891 40 (1981).
892 15 Lovitt, R. W., Kell, D. B. & Morris, J. G. The physiology of *Clostridium sporogenes* NCIB
893 8053 growing in defined media. *J Appl Bacteriol* **62**, 81-92 (1987).
894 16 Nemet, I. *et al.* A cardiovascular disease-linked gut microbial metabolite acts via
895 adrenergic receptors. *Cell* **180**, 862-877 e822, doi:10.1016/j.cell.2020.02.016 (2020).
896 17 Wildenauer, F. X. & Winter, J. Fermentation of isoleucine and arginine by pure and
897 syntrophic cultures of *Clostridium sporogenes*. *FEMS Microbiol Lett* **38**, 373-379 (1986).
898 18 Macy, J., Probst, I. & Gottschalk, G. Evidence for cytochrome involvement in fumarate
899 reduction and adenosine 5'-triphosphate synthesis by *Bacteroides fragilis* grown in the
900 presence of hemin. *J Bacteriol* **123**, 436-442, doi:10.1128/JB.123.2.436-442.1975
901 (1975).
902 19 Hess, V., Gonzalez, J. M., Parthasarathy, A., Buckel, W. & Muller, V. Caffeate
903 respiration in the acetogenic bacterium *Acetobacterium woodii*: a coenzyme A loop
904 saves energy for caffeate activation. *Appl Environ Microbiol* **79**, 1942-1947 (2013).
905 20 Bader, J. & Simon, H. ATP formation is coupled to the hydrogenation of 2-enoates in
906 *Clostridium sporogenes*. *FEMS Microbiol Lett* **20**, 171-175 (1983).
907 21 Tremblay, P. L., Zhang, T., Dar, S. A., Leang, C. & Lovley, D. R. The Rnf complex of
908 *Clostridium ljungdahlii* is a proton-translocating ferredoxin:NAD+ oxidoreductase
909 essential for autotrophic growth. *mBio* **4**, e00406-00412, doi:10.1128/mBio.00406-12
910 (2012).
911 22 Lovitt, R. W., Kell, D. B. & Morris, J. G. Proline reduction by *Clostridium sporogenes* is
912 coupled to vectorial proton ejection. *FEMS Microbiol Lett* **36**, 269-273 (1986).
913 23 Seedorf, H. *et al.* The genome of *Clostridium kluyveri*, a strict anaerobe with unique
914 metabolic features. *Proc Natl Acad Sci USA* **105**, 2128-2133 (2008).
915 24 Li, F. *et al.* Coupled ferredoxin and crotonyl coenzyme A (CoA) reduction with NADH
916 catalyzed by the butyryl-CoA dehydrogenase/Etf complex from *Clostridium kluyveri*. *J*
917 *Bacteriol* **190**, 843-850 (2008).
918 25 Buckel, W. & Thauer, R. K. Flavin-based electron bifurcation, a new mechanism of
919 biological energy coupling. *Chem Rev* **118**, 3862-3886 (2018).
920 26 Herrmann, G., Jayamani, E., Mai, G. & Buckel, W. Energy conservation via electron-
921 transferring flavoprotein in anaerobic bacteria. *J Bacteriol* **190**, 784-791 (2008).
922 27 Guo, C. J. *et al.* Depletion of microbiome-derived molecules in the host using *Clostridium*
923 genetics. *Science* **366**, doi:10.1126/science.aav1282 (2019).
924 28 Goodman, A. L. *et al.* Identifying genetic determinants needed to establish a human gut
925 symbiont in its habitat. *Cell Host Microbe* **6**, 279-289, doi:10.1016/j.chom.2009.08.003
926 (2009).
927 29 Wu, M. *et al.* Genetic determinants of in vivo fitness and diet responsiveness in multiple
928 human gut *Bacteroides*. *Science* **350**, aac5992, doi:10.1126/science.aac5992 (2015).
929 30 Medema, M. H., Takano, E. & Breitling, R. Detecting sequence homology at the gene
930 cluster level with MultiGeneBlast. *Mol Biol Evol* **30**, 1218-1223,
931 doi:10.1093/molbev/mst025 (2013).
932 31 Nayfach, S., Fischbach, M. A. & Pollard, K. S. MetaQuery: a web server for rapid
933 annotation and quantitative analysis of specific genes in the human gut microbiome.
934 *Bioinformatics* **31**, 3368-3370, doi:10.1093/bioinformatics/btv382 (2015).

935

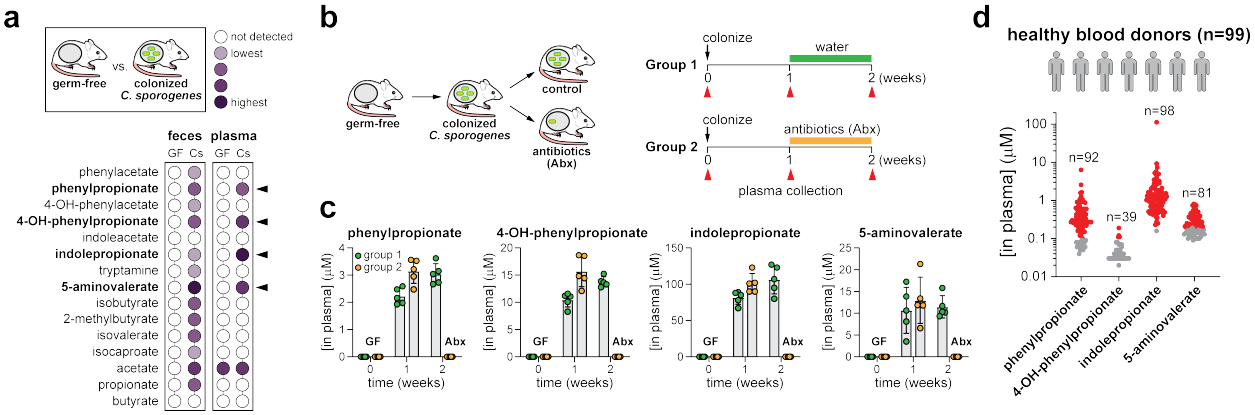

Figure 1. Microbial metabolism within the gut yields metabolites that circulate within the host. A) Fecal and plasma levels of metabolites in germ-free and *C. sporogenes* colonized mice. Data represent means of n = 5 mice. B) Experimental design for detecting metabolites in circulation of gnotobiotic mice before and after antibiotic treatment. C) Quantitation of phenylpropionate, 3-(4-hydroxyphenyl)propionate, indolepropionate, and 5-aminovalerate in plasma of gnotobiotic mice. Abx, antibiotics. D) Quantitation of phenylpropionate, 3-(4-hydroxyphenyl)propionate, indolepropionate, and 5-aminovalerate in plasma of healthy human blood donors (n = 99). Numbers above plots indicate the total number of individuals with detectable metabolite levels. Red dots indicate concentrations within the accurate measurable range of the assay, and gray dots are detected but below the lower limit of quantitation. Concentrations of metabolites detected in mice (A and C) are provided in **Supplementary Tables 1-4** and in humans (D) are provided in **Supplementary Table 5**.

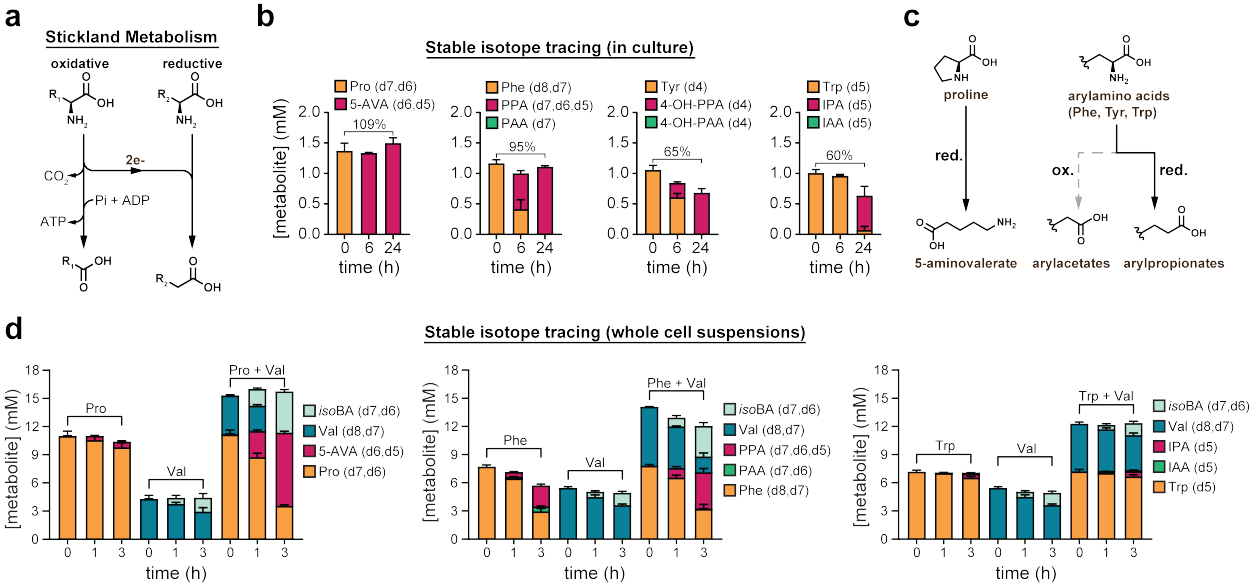

Figure 2. Circulating metabolites are formed from reductive pathways for Stickland metabolism. A) Overview of the Stickland Reaction. Amino acids are metabolized as pairs, with one being oxidized while the other is reduced. The oxidative pathway forms ATP via substrate level phosphorylation and the reductive pathway serves redox balance. B) Stable isotope tracing. *C. sporogenes* was cultured in a synthetic medium containing 20 amino acids where Phe, Tyr, Trp, and Pro were individually substituted by their deuterium isotopologues. Cell-free supernatants (n = 3 per group) were collected at t = 0, 6, 24 h and metabolites were detected by LC-MS. C) End products of Pro, Phe, Tyr, Trp are reductive Stickland metabolites. D) Stable isotope tracing of *C. sporogenes* cell suspensions incubated with oxidative (Val) and reductive (Pro, Phe, Trp) amino acid pairs. 5-AVA, 5-aminovalerate; PPA, phenylpropionate; PAA, phenylacetate; 4-OH-PPA, 3-(4-hydroxyphenyl)propionate; 4-OH-PAA, 4-hydroxyphenylacetate; IPA, indolepropionate; IAA, indoleacetate; *iso*BA, isobutyrate.

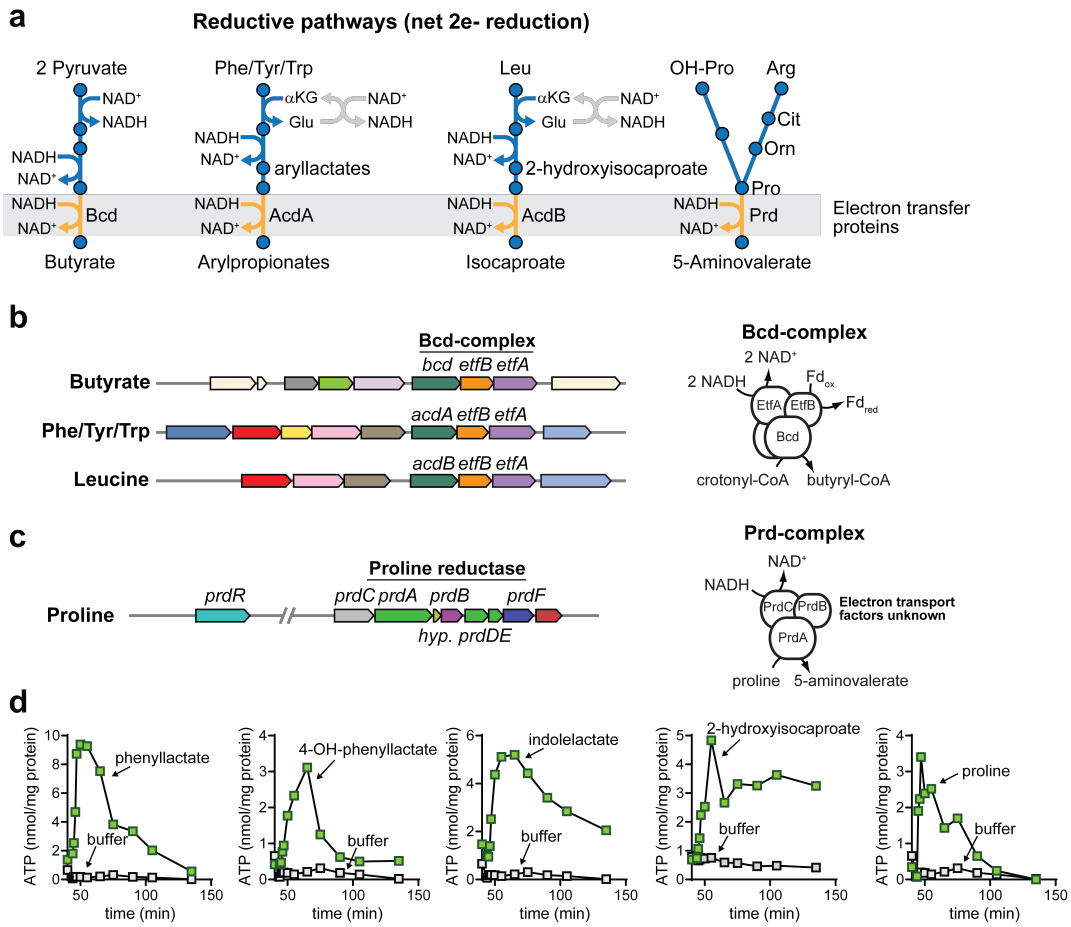

968

969 **Figure 3. Reductive metabolism is coupled to ATP formation.** A) Pathways for
970 reductive Stickland metabolism catalyze net 2 electron reductions and each converges
971 on an electron transfer protein. B) Gene clusters for reductive metabolism of Phe, Tyr,
972 Trp, and Leu share homologs of the electron bifurcating butyryl-CoA dehydrogenase
973 complex (Bcd) which produces reduced ferredoxin. C) The proline metabolism gene
974 cluster encodes components of the proline reductase enzymes which is implicated in
975 proline-dependent extracellular proton transport. D) Reductive metabolism of Phe, Tyr,
976 Trp, Leu, and Pro are coupled to ATP formation in *C. sporogenes* resting cell
977 suspensions. For Phe, Tyr, and Trp, intermediates in the reductive pathways (e.g.,
978 phenyllactate, 3-(4-hydroxyphenyl)lactate, and indolelactate) were used. For D,
979 experiments were repeated independently three times and representative data are
980 shown.

981

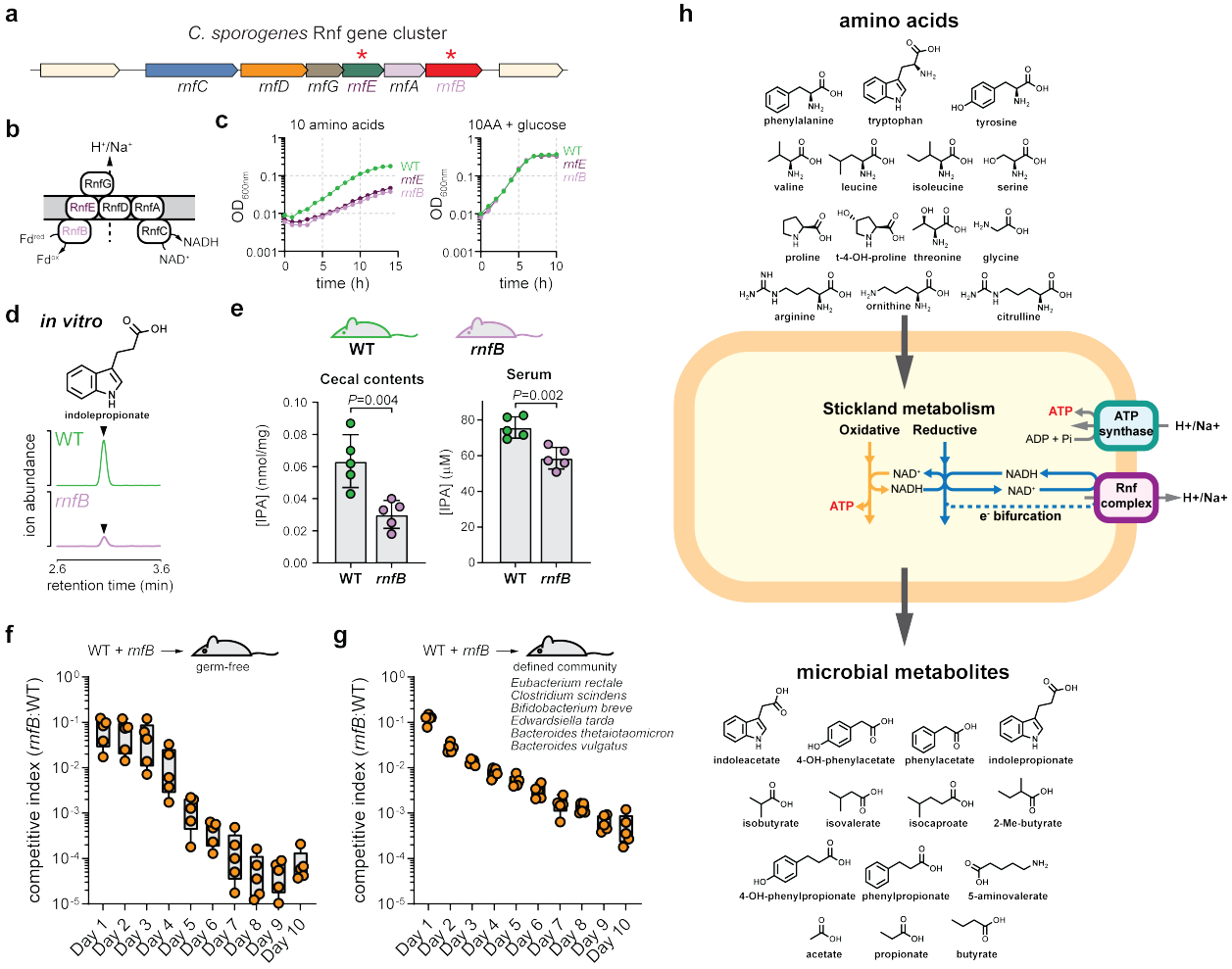

Figure 4. The Rnf complex is important for amino acid metabolism and is a key fitness determinant in vivo. A) The *C. sporogenes* Rnf complex gene cluster. B) Model for the membrane bound Rnf complex which generates a proton or sodium motive force by shuttling electrons from reduced ferredoxin to NAD^+. C) The *rnfB* and *rnfE* mutants suffer a growth defect in amino acid medium that can be restored by addition of glucose. D) The *rnfB* mutant produces less indolepropionate during growth in defined medium with 10 amino acids. E) Mice mono-colonized with the *rnfB* mutant accumulate less indolepropionate in feces and in plasma. F) The *rnfB* mutant exhibits an *in vivo* competition defect in gnotobiotic mice in the context of mono-colonization and G) a more complex defined microbial community. H) Revised model for Stickland metabolism and its contribution to gut bacterial derived metabolites. For C-D, experiments were repeated independently three times and representative data are shown. For E-G, Box and whisker plots show median values, 25th–75th percentiles and range for $n = 5$ biological replicates. IPA, indolepropionate.